

PNNL-37070

# **Embedded Aluminum Nitride Sensors for Advanced Reactors**

November 2024

Saumyadeep Jana Amrita Lall Tiffany Kasper Shawn Riechers Ryan Meyer Zack Kennedy Michelle Fenn Ken Ross



#### DISCLAIMER

This report was prepared as an account of work sponsored by an agency of the United States Government. Neither the United States Government nor any agency thereof, nor Battelle Memorial Institute, nor any of their employees, makes any warranty, express or implied, or assumes any legal liability or responsibility for the accuracy, completeness, or usefulness of any information, apparatus, product, or process disclosed, or represents that its use would not infringe privately owned rights. Reference herein to any specific commercial product, process, or service by trade name, trademark, manufacturer, or otherwise does not necessarily constitute or imply its endorsement, recommendation, or favoring by the United States Government or any agency thereof, or Battelle Memorial Institute. The views and opinions of authors expressed herein do not necessarily state or reflect those of the United States Government or any agency thereof.

PACIFIC NORTHWEST NATIONAL LABORATORY

operated by

BATTELLE

for the

UNITED STATES DEPARTMENT OF ENERGY

under Contract DE-AC05-76RL01830

Printed in the United States of America

Available to DOE and DOE contractors from the Office of Scientific and Technical Information, P.O. Box 62, Oak Ridge, TN 37831-0062

ph: (865) 576-8401 fox: (865) 576-5728 email: reports@osti.gov

Available to the public from the National Technical Information Service 5301 Shawnee Rd., Alexandria, VA 22312 ph: (800) 553-NTIS (6847) or (703) 605-6000

email: <a href="mailto:info@ntis.gov">info@ntis.gov</a>
Online ordering: <a href="http://www.ntis.gov">http://www.ntis.gov</a>

## **Embedded Aluminum Nitride Sensors for Advanced Reactors**

November 2024

Saumyadeep Jana Amrita Lall Tiffany Kasper Shawn Riechers Ryan Meyer Zack Kennedy Michelle Fenn Ken Ross

Prepared for the U.S. Department of Energy under Contract DE-AC05-76RL01830

Pacific Northwest National Laboratory Richland, Washington 99354

#### **Abstract**

This project aims to manipulate the of growth of aluminum nitride (AIN) inclusions in an iron-chromium-aluminum (FeCrAl) alloy, using the principle of powder metallurgy and heat treatment methods. to promote the formation of AIN phase within FeCrAl for embedded sensing. This effort seeks to fill in a gap with respect to robust sensor hardware for ubiquitous structural health monitoring of advanced nuclear reactors. A systematic evaluation of various solid-state methods will be performed to understand the influence of process conditions on AIN growth and to promote the growth of desirable AIN phase. Fabricated specimens will be analyzed to investigate the AIN structures that are formed using a suite of tools to characterize the concentration, morphology, and distribution of AIN within the FeCrAl substrate.

Abstract

#### **Summary**

This study investigated the methods to grow aluminum nitride (AIN) crystals in-situ within a structural alloy matrix. AIN is a sensor material with piezo electric response that is active up to 1000C. FeCrAl has been selected as the alloy of interest, since it contains AI in solid solution. Oxide dispersion strengthened FeCrAl alloys are highly relevant for nuclear applications, especially for advanced reactors. Powder metallurgy techniques have been pursued for AIN crystal growth. It was noted that AIN phase can be generated within FeCrAl matrix, when heated under N<sub>2</sub> environment. However, fabrication of composite AIN + FeCrAl coupons were not successful. This is related to the requirement of very high temperature sintering needed for AIN phase. Use of solid-state reaction was partially successful in forming AIN in alloys that do not contain AI as an alloying element. This could be achieved by converting AIB<sub>2</sub> into AIN in a 316L stainless steel matrix. Thin film growth through laser sputtering appeared to give the best results.

Piezo electric behavior of in-situ grown AIN crystals were measured using piezo force microscopy (PFM), which is an adaptation of atomic force microscopy (AFM). Piezo response was linked to measurement of d33 property. In-situ grown AIN phase did not show high d33 values, since AIN crystal orientation was mostly random in nature. In comparison, better d33 values were noted in thin film AIN fabricated by laser sputtering.

Based on the current observation, AIN integration to a structural alloy would be better achieved by coming up with innovative ceramic to metal joining methods, for future research.

Summary

#### **Acknowledgments**

This research was supported by the **Energy Mission Seed Investment**, under the Laboratory Directed Research and Development (LDRD) Program at Pacific Northwest National Laboratory (PNNL). PNNL is a multi-program national laboratory operated for the U.S. Department of Energy (DOE) by Battelle Memorial Institute under Contract No. DE-AC05-76RL01830.

Acknowledgments

#### **Contents**

Abstra	act		ii		
Summ	ary		iii		
Ackno	wledgi	ments	iv		
1.0	Introd	luction	1		
2.0	Expe	rimental Procedure	2		
3.0	Results				
	3.1	Use of heat treatment to grow AIN phase in-situ	3		
	3.2	Use of powder metallurgy to fabricate AIN + FeCrAl composite	4		
	3.3	Use of reaction sintering to form AIN in-situ	8		
	3.4	Use of thin film deposition method to grow AIN film	9		
	3.5	Use of piezo force microscopy (PFM) for piezo property measurement	10		
4.0	Conc	lusion	13		
5.0	Refer	ences	14		
Figu	ıres				
Figure	1. SE	M image of the FeCrAl coupon after heat treatment:	4		
Figure	2. ED	PS elemental mapping confirms blocky phase as AIN, when FeCrAI disc is heat treated under $N_2$ environment	4		
Figure	: 3. Op	otical micrograph of FeCrAl powder mixed with AIN powder, sintered at	5		
Figure	4. Te	mperature and pressure profile for pure AIN sintering at 1850C, 4 h	5		
Figure	5. Pc	wder size distribution of AIN powder, (a) As-received, (b) after milling	5		
Figure	6. Pu	re AIN pellets and FFF-printed coupons after sintering	6		
Figure	7. Mic	rographs of FFF-printed and sintered coupons;	7		
Figure	8. Mic	rostructure of pure AIN after milling;	7		
Figure	9. Mic	rostructure of pure AIN after milling and with sintering additives;	7		
Figure	10. E	OS elemental map of AIN with sintering additives confirms presence of Y <sub>2</sub> O <sub>3</sub> and CaCO <sub>3</sub>	8		
Figure	11. S	olid state chemical reaction explored for converting AIB <sub>2</sub> to AIN in-situ	8		
Figure	12. G	IXRD patterns of AIN thin films deposited by PLD	10		
Figure	13. P	TM response of AIN thin films.	11		
Tab	les				
Table	1. Deta	ails of heat treatment scheme tried on FeCrAl discs	3		
Table	2. PLC	deposition conditions for AIN films deposited on fused silica substrates	9		
Table	3.Sum	mary of PFM measurement carried on select samples	12		

Contents

#### 1.0 Introduction

Aluminum nitride (AIN) is one of a few materials with potential to offer a piezoelectric function in harsh environments which provides potential in-situ sensor capabilities<sup>1</sup>. The key question this effort seeks to answer is: How can we develop methods to embed AIN phase in a structural alloy of interest for remote sensing. We have selected FeCrAl as the structural alloy for this study. Other key questions to address include characterizing the integrity of the bond between the AIN and surrounding FeCrAl substrate and the impact of the AIN formations on the mechanical integrity of the overall structure.

The ability to inspect the structural integrity of structures within nuclear power plants is crucial to maintaining their safe operation for extended periods. Ultrasonic testing plays a major role in maintaining the current fleet of operating light-water reactors through inspections conducted periodically during outages. For many advanced reactor concepts, these inspections will need to be performed at significantly elevated temperatures while the reactor is operating to accommodate online refueling or to prevent the coolant from freezing during outages. The development of ultrasonic sensors capable of surviving in advanced reactor harsh environments is an active area of investigation<sup>1-3</sup>. Some key challenges include the basic tolerance of the sensor materials to the relevant environment, as well as the integrity of joints formed between various sensor subcomponents and between sensors and the structures to be surveilled<sup>1-3</sup>. AlN has excellent physical and chemical properties such as high hardness, corrosion resistance, mechanical strength, high electrical resistivity, and thermal stability<sup>1-3</sup>.

Introduction 1

#### 2.0 Experimental Procedure

AlN is a non-oxide ceramic with a list of unique physical properties. For structural health monitoring through remote sensing, piezoelectric properties are of interest in a sensor material. AlN exhibits piezoelectricity, meaning it generates an electrical charge in response to mechanical stress. This makes it highly suitable for applications such as **pressure sensors**, **strain sensors**, **and accelerometers**. In these sensors, the deformation of the AlN material due to applied force or vibration results in an electrical signal that can be measured.

Compared to other piezoelectric materials such as PZT, AlN can offer piezoelectric properties at a temperature up to 1000C or higher. Most other piezoelectric material loses their sensing capability above 300-400C. High temperature piezoelectric properties observed in AlN makes it particularly interesting for use as sensor material in advanced nuclear reactors that are designed to operate at higher temperature (>600C) and in some cases, harsh chemical environments.

Currently, there are no known methods to bond AIN sensor to the underlying structural alloy substrate. Some tried methods include thin film deposition, adhesive bonding etc. In this research, we investigated methods to grow AIN phase in-situ in a structural alloy of interest.

FeCrAl has been selected as the structural alloy. FeCrAl alloy, when strengthened with oxide dispersion nano particles, can show attractive mechanical properties and corrosion resistance for use in harsh environments. In this research, we looked at methods to create AlN phase within FeCrAl matrix. Synthesis of AlN phase has been attempted using following methods listed below:

- 1. Use of heat treatment to form AIN crystals in-situ through precipitation in structural alloys.
- 2. Use of powder metallurgy (PM) to form AIN + structural alloy composite and explore feasibility of solid-state additive manufacturing (SSAM) to create AIN coupons.
- 3. Use of reaction sintering to form AlN crystals in a structural alloy.
- 4. Use of thin film deposition to grow AIN film.

#### 3.0 Results

This study primarily used the concept of powder metallurgy to investigate growth of AIN phase. Therefore, formation of AIN phase through solid state reactions was the major focus of this research. As outlined in the experimental section, methods to grow AIN phase was attempted by developing heat treatment procedures, sintering conditions etc. Following subsections report our findings for different methodologies tried.

#### 3.1 Use of heat treatment to grow AIN phase in-situ

The main synthesis methods for AIN are carbothermal reduction, chemical vapor deposition (CVD), and direct nitridation. Direct nitridation is a key method for the commercial production of AIN powders from metallic AI powder. This cost-effective technique uses a straightforward nitridation system. Full nitridation is typically achieved at temperatures up to 1500 °C with flowing nitrogen-based gases. However, this process often leads to agglomeration of AIN powders due to the low melting point of aluminum, which is lower than the temperature needed for nitridation.

We explored the direct nitridation method to grow AIN phase in-situ in a metallic alloy. FeCrAl alloy, a ferritic stainless steel, has been used for this study. The FeCrAl alloy used in this study contains 20 wt.% Cr, 5 wt.% AI, and rest Fe. Since there is a good amount of AI in solid solution, we explored the possibility of converting AI into AIN by heat treatment. Following heat treatment schemes were employed, as noted in Table 1.

Table 1. Details of fleat treatment scheme thed off rectal discs									
Heat treatment #	Temp	Time	Environment	Status	AIN				
1	1000C	2 h	air	No wt gain	Negligible amount				
2	1100C	12 h	air	1.15% wt gain	Negligible amount				
3	1100C	48 h	air	1.13% wt gain	Negligible amount				
4	1000C	139 h	N <sub>2</sub>	3.02% wt gain	Large, blocky				
5	1100C	48 h	$N_2$	1.7% wt gain	Large, blocky				
6	1100C	120 h	N <sub>2</sub>						

Table 1. Details of heat treatment scheme tried on FeCrAl discs.

As summarized in Table 1, FeCrAl discs show higher weight gain when heat treated under flowing  $N_2$ , compared to air. There is an effect of heat treatment time as well, with longer time leading to higher weight gain. This behavior indicates solid state reaction happening in FeCrAl matrix, when heated under  $N_2$ . SEM imaging was carried out to check for the formation of AlN crystals within FeCrAl matrix after high temperature heat treatment.

Fig. 1 shows a comparison between air vs.  $N_2$  heat treatment when FeCrAl coupons are heated to 1100C for 48 h. FeCrAl matrix remains unchanged, and presence of large equiaxed grains are observed when heat treatment is carried out in air (Fig. 1a). however, the same FeCrAl matrix shows formation of large, blocky phase when heat treated under  $N_2$ . EDS elemental mapping was carried out on  $N_2$  heat treated FeCrAl sample. EDS elemental map data is shown in Fig.2, which conclusively proves those blocky phases to be AIN. Therefore, it appears that heat treatment of FeCrAl alloy under flowing  $N_2$  is an effective method to create AIN phase insitu.

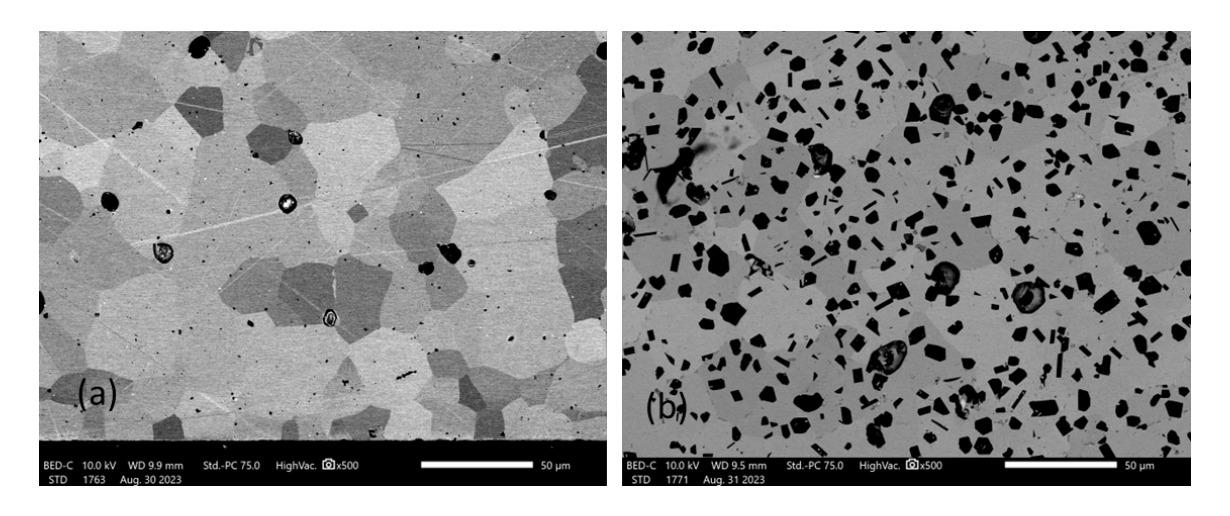


Figure 1. SEM image of the FeCrAl coupon after heat treatment: at, (a) 1100C, 48 h, air; and (b) 1100C, 48 h, N<sub>2</sub>, numerous AIN phase has formed.

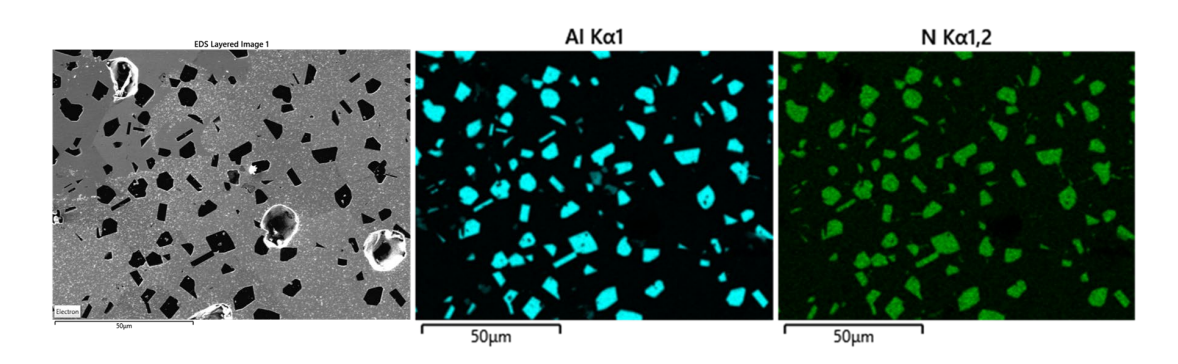


Figure 2. EDS elemental mapping confirms blocky phase as AIN, when FeCrAl disc is heat treated under  $N_2$  environment.

#### 3.2 Use of powder metallurgy to fabricate AIN + FeCrAl composite

Commercially available AIN powder was mixed with FeCrAI powder, and later sintered at high temperature to create a composite sample. The idea behind this approach was to explore the possibility of making composites containing AIN, where AIN quantity can be tailored to the need of a user. Afterwards these composites could be inserted as sensor material into a substrate structural alloy, at the places of interest.

An example of AIN + FeCrAl composite coupon, after sintering at 1350C for 6 h, is shown in Fig. 3. The composite coupon, shown in this optical micrograph, has AIN mixed with FeCrAl in a 1:1 ratio by weight. Since density of AIN is 3.26 g/cc, and density of FeCrAl is 7.15 g/cc, the volume fraction of AIN phase in the shown composite is ~ 70%. Bright phases, shown by the arrow represents FeCrAl particle. Lack of sintering is evident in this sample. This is because of the high temperature required for sintering AIN phase. Overall, fabrication of composite coupons by traditional powder metallurgy route was not successful.

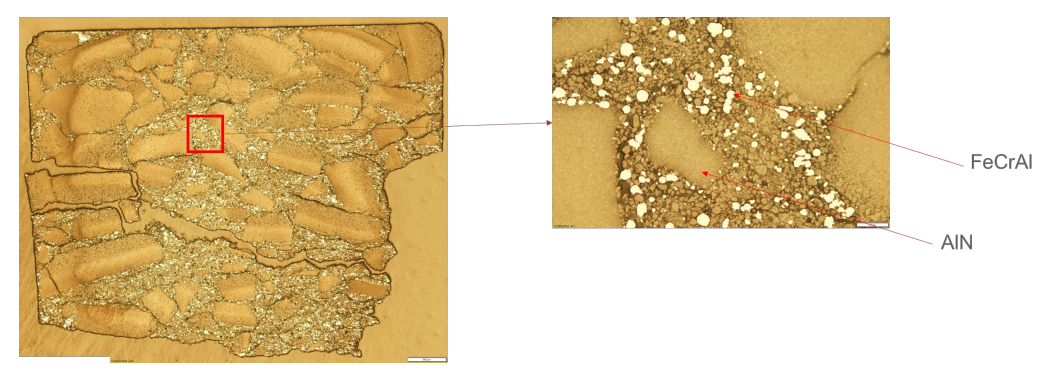


Figure 3. Optical micrograph of FeCrAl powder mixed with AlN powder, sintered at 1350C.

For benchmarking purpose, commercially available AIN powder was pressed into cylindrical shaped pellets and sintered at 1850C for 4 h. For AIN sintering, small amounts of sintering aids such as CaCO<sub>3</sub>, Y<sub>2</sub>O<sub>3</sub> were added with AIN powder to achieve better densification. Temperature profile of the sintering run for pure AIN powder is shown in Fig. 4. Since, smaller particle size leads to better densification, as-received AIN powder was milled at PNNL, and later sintered. Powder size distribution of AIN powder in as-received (AR) and after milling, is reported in Fig. 5. Milling resulted in significant particle size reduction, with D90 value becoming ~50% less than AR particle size.

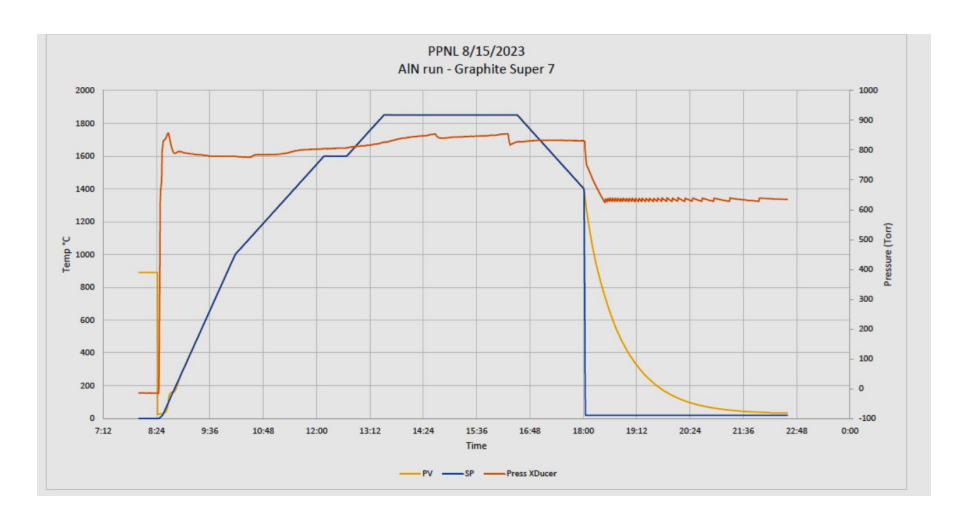


Figure 4. Temperature and pressure profile for pure AIN sintering at 1850C, 4 h

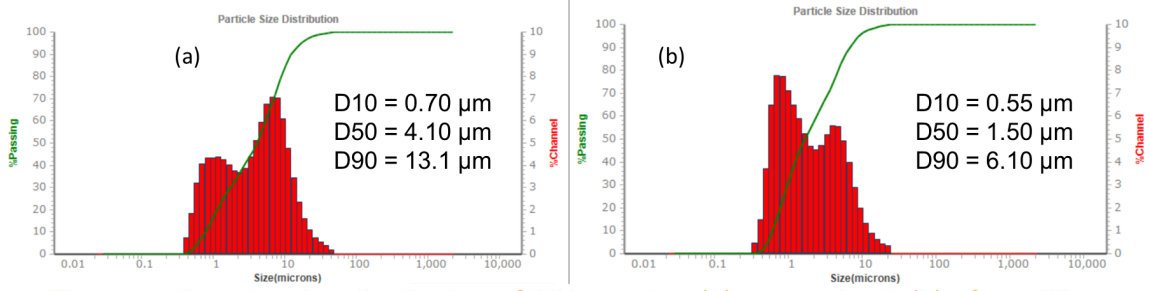


Figure 5. Powder size distribution of AIN powder, (a) as received, (b) after milling

Solid state additive manufacturing (SSAM) of AIN was also tried, using fused filament fabrication (FFF) method. AIN powder was mixed with appropriate polymeric binders to create a filament, which was later used to print small test coupons (25 x 7 x 3 mm). Fig. 6 shows images of pressed pellets, and FFF-fabricated coupons after sintering. Pellets, which were 6 mm tall in height, mostly retained their shapes. However, FFF-printed coupons show some degree of warping, which is due to binder burnout and related effect on final shape.

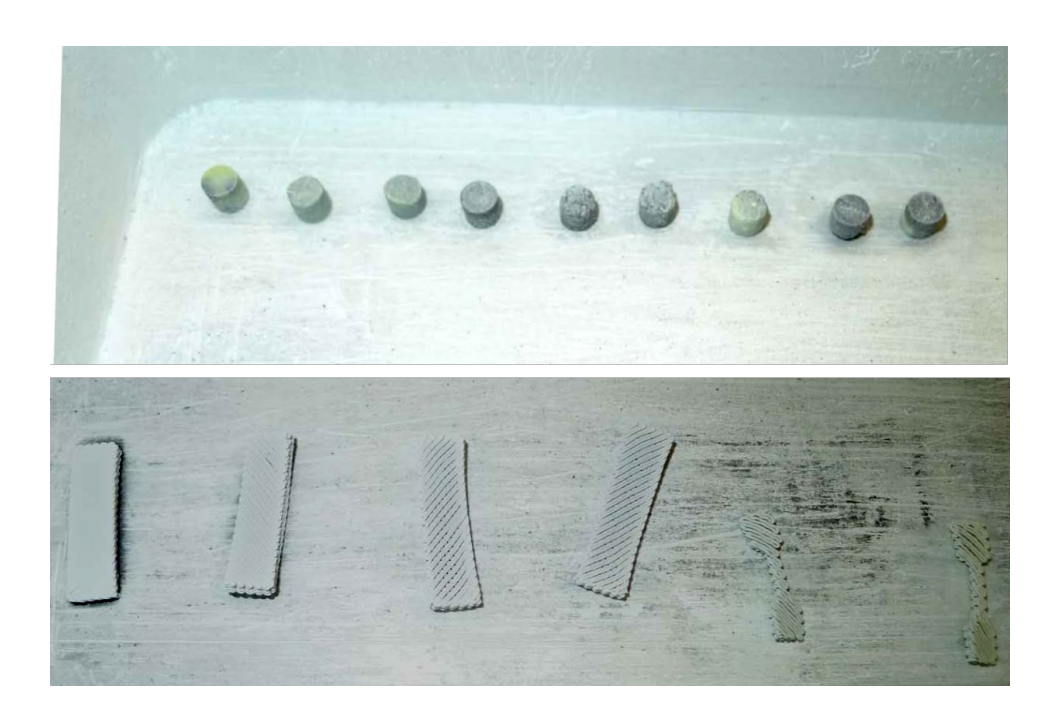


Figure 6. Pure AIN pellets and FFF-printed coupons after sintering

Microstructure and chemical composition of sintered AIN samples were examined by SEM and EDS method. Fig. 7 shows cross-section image of FFF-fabricated AIN coupon after sintering, at various magnifications. AIN powder in AR condition was used for printing these coupons. Low-magnification image of the printed coupon in thickness direction shows that it is possible to create dense layers by FFF method, with minimal defects (Fig. 7a). Large voids between vertical layers are a common printing-induced defect experienced in FFF-based SSAM method. However, at a higher magnification, presence of large porosities could be noticed, which indicate incomplete sintering, and therefore, lack of densification (Fig. 7b and 7c). Further process optimization, such as use of a finer grade of AIN powder for filament fabrication, FFF printing process optimization, and sintering time and temperature modification is required to obtain fully dense AIN coupon after FFF-based fabrication.

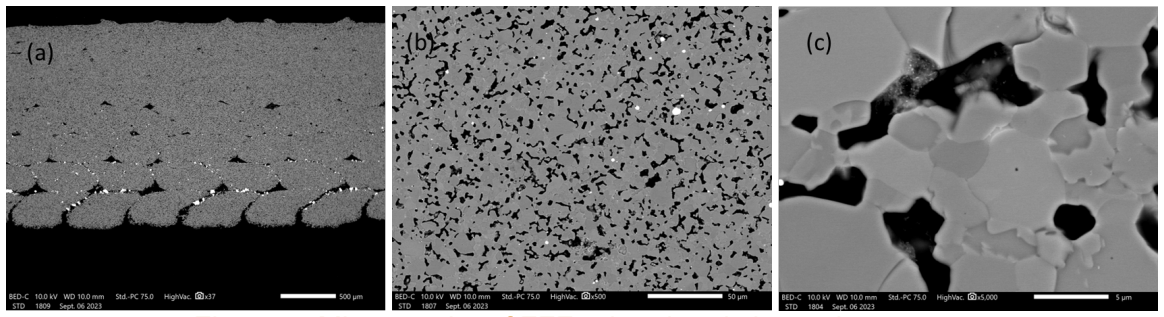


Figure 7. Micrographs of FFF-printed and sintered coupons;
(a) low-magnification overview, (b) intermediate magnification shows porosity, (c) high magnification captures grain structure.

For comparison, microstructure of pressed and sintered pellets made using (i) milled AIN powder, and (ii) milled AIN powder + sintering aid are shown in Fig. 8 and Fig. 9. Milling of AIN powder results in better densification after sintering (Fig. 8a). Higher magnification image of milled AIN powder sintered sample shows irregular morphology (Fig. 8b), which is most likely induced by milling event. Milled AIN powder with addition of sintering aids also shows good densification behavior (Fig. 9a). Presence of sintering aids are mostly noted along the AIN grain boundaries, and there is a distinct change in the shape of AIN grains when sintering aids are used (Fig. 9b).

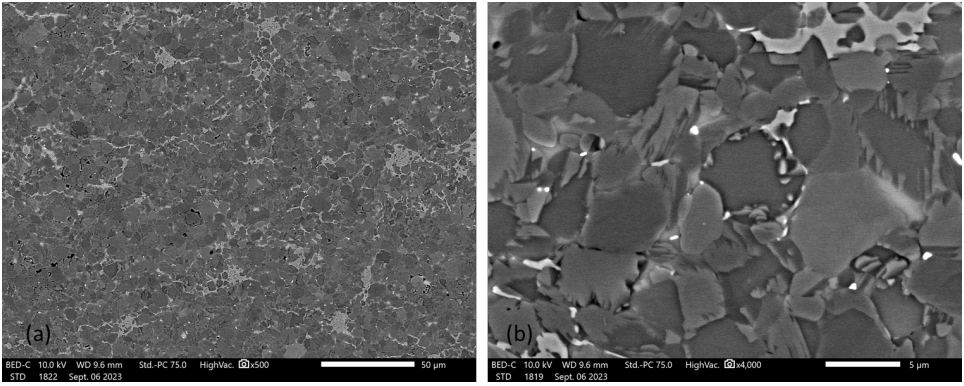


Figure 8. Microstructure of pure AIN after milling; (a) low-magnification, (b) high magnification showing irregular grain morphology

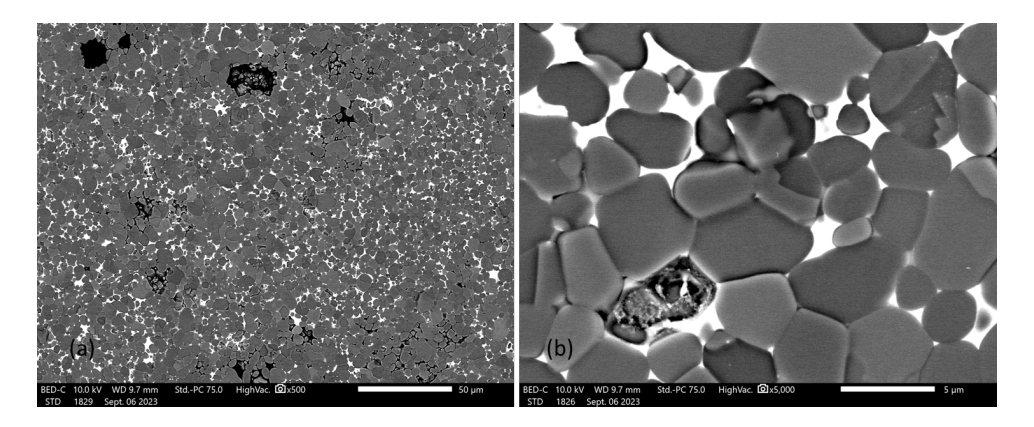


Figure 9. Microstructure of pure AIN after milling and with sintering additives; (a) low-magnification, (b) high magnification showing rounded grain morphology

EDS elemental mapping of sintered pellet made by AIN powder with sintering aids is captured in Fig. 10. Good densification is apparent, in comparison to sintering behavior of AR AIN powder, shown in Fig. 7b and 7c. Y<sub>2</sub>O<sub>3</sub> and CaCO<sub>3</sub> has been used as sintering aids, confirmed by EDS elemental mapping. Sintering aids are uniformly present in the AIN matrix.

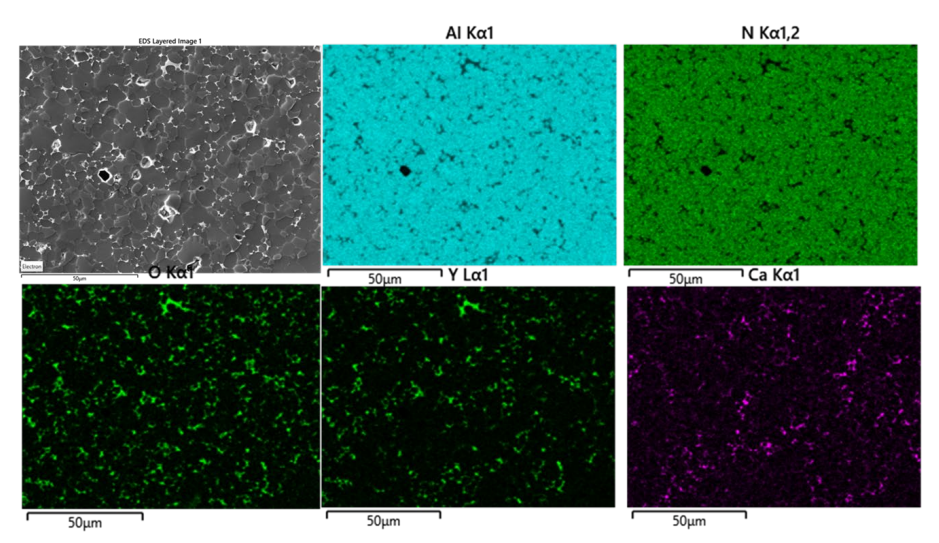


Figure 10. EDS elemental map of AIN with sintering additives confirms presence of Y<sub>2</sub>O<sub>3</sub> and CaCO<sub>3</sub>

#### 3.3 Use of reaction sintering to form AIN in-situ

During initial phase of this study, we used FeCrAl as our candidate structural alloy for in-situ formation of AlN phase. Since FeCrAl contains Al in solid solution, it was first choice as a structural alloy. However, austenitic stainless steels such as 304L SS, 316 L SS are common structural alloys used in the nuclear energy sector. Therefore, we explored the possibility of forming AlN phase in a stainless-steel matrix using solid state method.

We specifically studied the reaction sintering route, where we aimed to convert a non-nitride compound to AlN by solid state reaction. Following chemical reaction has been explored (Fig. 11). 316L SS powder (70% by vol.) was mixed with AlB2 powder (30% by vol.), and was heat treated in  $N_2$  environment at 1100C for 120 h. The composite sample did show formation of AlN. However, the solid-state reaction route needs significant process optimization to generate reasonable amount of AlN for effective piezo response.

$$22AlB_2 + 9.33N_2 \rightarrow 18.66AlN + 2Al_{1.67}B_{22} (1000 \text{ °C}),$$

$$Al_{1.67}B_{22} + N_2 \rightarrow BN + AlN (>1400 \,^{\circ}C).$$

Figure 11. Solid state chemical reaction explored for converting AIB<sub>2</sub> to AIN in-situ

#### 3.4 Use of thin film deposition method to grow AIN film

Aluminum nitride (AIN) thin films were synthesized by pulsed laser deposition (PLD). A KrF excimer laser (248 nm wavelength) operated at 10 Hz was directed on an AIN ceramic target (K.J. Lesker, Inc.) at a repetition rate of 10 Hz in a background gas of 10 mTorr N<sub>2</sub>. The ablated target material was captured on fused silica, or 301 stainless steel (SS) substrates held at 800°C.

Grazing incidence X-ray diffraction (GIXRD, Rigaku SmartLab) was utilized to evaluate the crystallinity of the resulting AIN thin films. As tabulated in Table 2 and shown in Fig. 12(a, c), the AIN films deposited on fused silica at a substrate temperature of  $800^{\circ}$ C were amorphous under higher  $N_2$  background pressure (10 mTorr and 20 mTorr) and weakly crystalline under lower  $N_2$  background pressure of 1 mTorr. From these results,  $800^{\circ}$ C and 1 mTorr  $N_2$  were chosen as optimum deposition parameters for AIN thin films.

The amorphous AIN films were treated similarly to the SS alloys studied elsewhere in the project that developed AIN inclusions after heat treatment in an  $N_2$  atmosphere. The amorphous AIN films were annealed in an  $N_2$  atmosphere at 1100°C for 120 hrs. This thermal treatment did not result in crystalline AIN, although the conditions were sufficient to crystallize the fused silica into cristobalite and quartz (Fig. 12(b)). Magnetite (Fe<sub>3</sub>O<sub>4</sub>) was also observed but was attributed to contaminant powders acquired during the anneal.

Table 2. PLD deposition conditions for AIN films deposited on fused silica substrates. Film crystallinity was assessed by GIXRD.

Substrate temperature	N₂ flow rate / pressure	Film crystallinity
800°C	10 sccm / 10 mTorr	Amorphous
800°C	10 sccm / 25 mTorr	Amorphous
800°C	10 sccm / 1 mTorr	Weakly crystalline

To mimic the AIN inclusions in SS studied elsewhere in the project, AIN thin films were deposited on polished 301 SS substrates under optimized conditions of  $800^{\circ}$ C substrate temperature and 1 mTorr N<sub>2</sub> pressure. These AIN thin films were confirmed to be partially crystalline by GIXRD, as shown in Fig. 12(d).

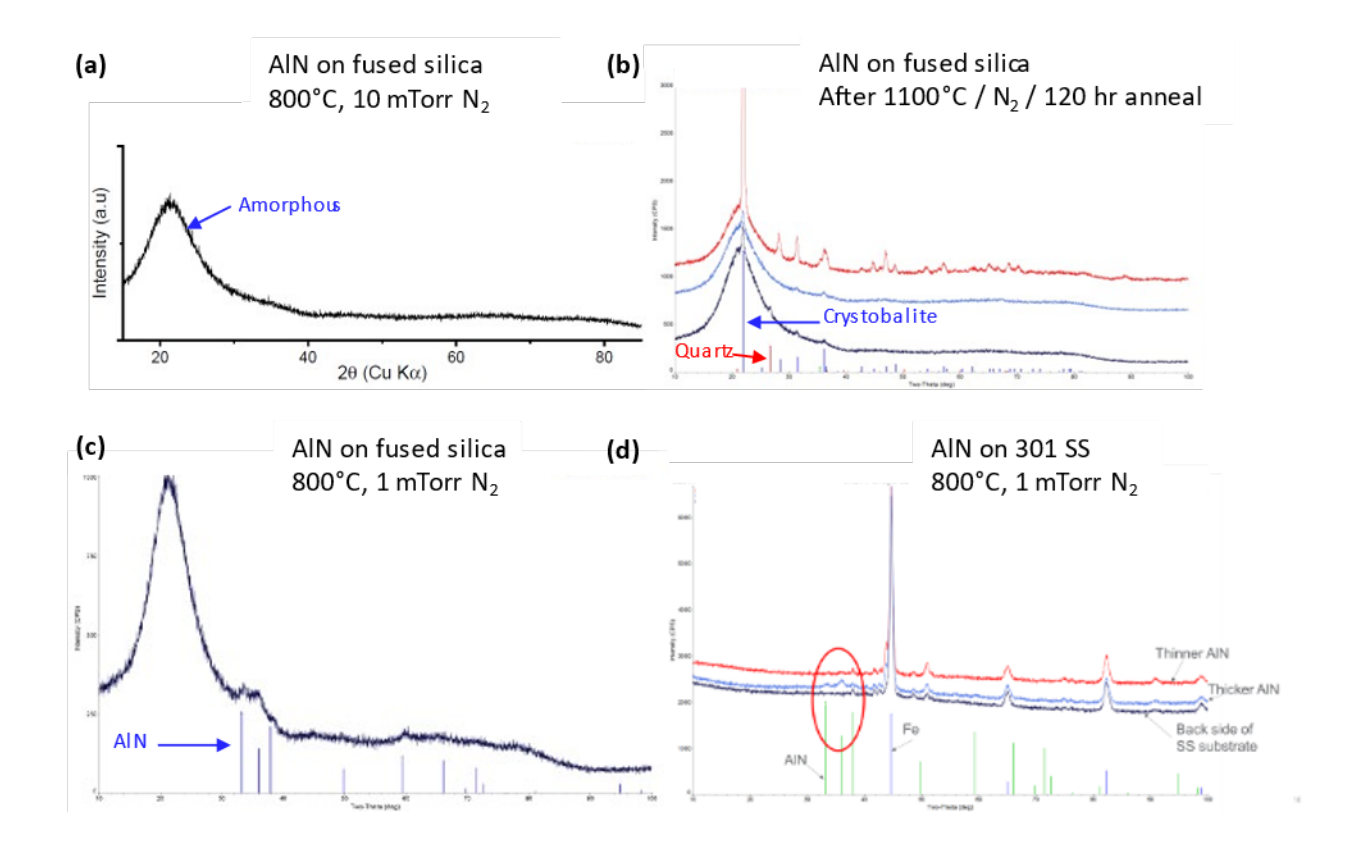


Figure 12. GIXRD patterns of AIN thin films deposited by PLD.

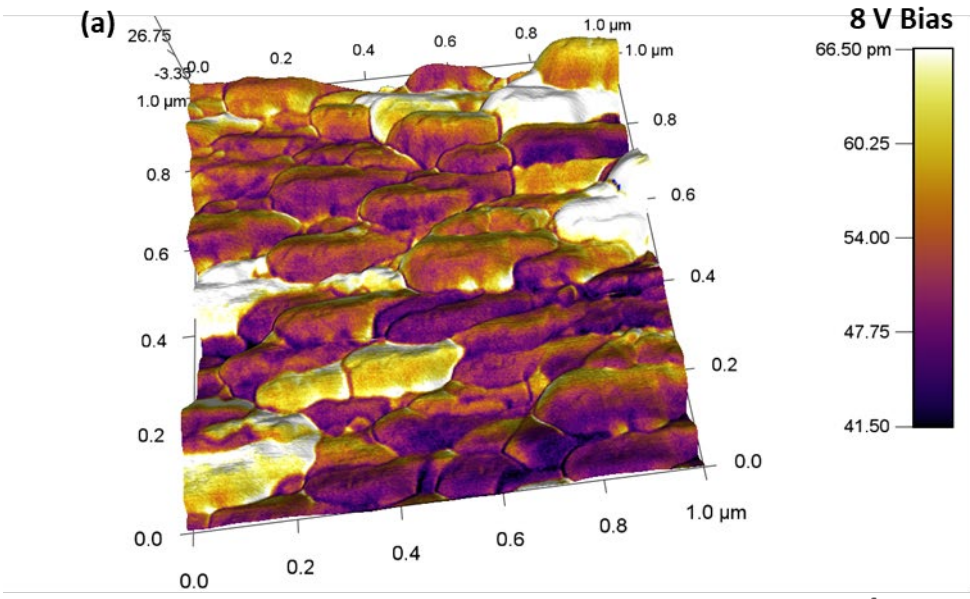
(a) Amorphous AIN deposited on fused silica at 800°C, 10 mTorr N<sub>2</sub>. (b) Amorphous AIN thin films after annealing in N<sub>2</sub> atmosphere at 1100°C for 120 hrs. (c) Weakly crystalline AIN deposited on fused silica at 800°C, 1 mTorr N<sub>2</sub>. (d) Weakly crystalline AIN deposited on 301 SS at 800°C, 1 mTorr N<sub>2</sub>.

### 3.5 Use of Piezoresponse force microscopy (PFM) for piezo property measurement

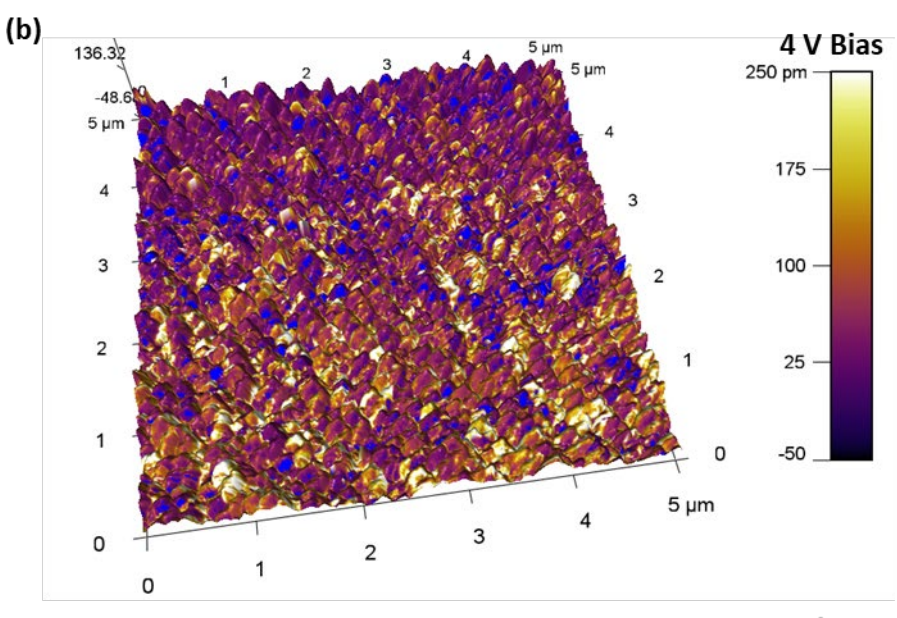
Piezoresponse force microscopy (PFM) in conjunction with atomic force microscopy (AFM, Asylum MFP-3D) was utilized to evaluate the piezoelectric properties of the AlN thin films. Piezo response is measured as d33, where larger values of  $d_{33}$  indicate a stronger response. The piezo response of the AlN thin films is summarized in Fig. 13. Weakly crystalline AlN thin films deposited on both fused silica and 301 SS exhibited a measurable piezo response. The response of the AlN film on 301 SS,  $d_{33}$  = 14.2 pm/V, was two times the response of the AlN film on fused silica ( $d_{33}$  = 6.7 pm/V). However, it should be noted that the film thicknesses were not established, and it might be expected that thicker films would exhibit a stronger piezo response than thinner films.

A comprehensive summary of PFM measurement analysis carried on select samples that contained AlN phase is reported in Table 3. It appears that the best piezo response is noted for pure AlN material, in as-sintered condition. PFM measurement method has been benchmarked by using a standard BiTiO3 reference. Piezo response of pure AlN, although in poly crystalline

form, appears to be quite high (73 pm/V). AIN phase, grown in-situ within FeCrAl alloy by heat treatment does show piezo response as well, although the magnitude of the response remains low (9.9 pm/V).



Average piezo response:  $d_{33} = 6.7 \text{ pm/V}$ 



Average piezo response:  $d_{33} = 14.2 \text{ pm/V}$ 

Figure 13. PFM response of AIN thin films.

(a) Overlay of topography (from AFM) and piezoresponse (from PFM) for weakly crystalline AIN thin film deposited on fused silica. (b) Overlay of topography and piezoresponse for weakly crystalline AIN thin film deposited on 301 SS.

Table 3.Summary of PFM measurement carried on select samples.

Sample composition	PFM		
Sample composition	Bias, V	d33 pm/V	
FeCrAI, NO AIN	10	0.88	
BiTiO, Reference	0.5	89	
33% by vol AIN +67%316L+2 wt.% Y <sub>2</sub> O <sub>3</sub>	1	8	
33% by vol AIN + 67% FeCrAI + 2 wt.% Y <sub>2</sub> O <sub>3</sub>	2	4	
50% by vol AIN 50% by vol FeCrAI	5	6	
Sintered FeCrAl disc Heat treated at 1100C for 120h under N <sub>2</sub>	4	9.9	
100% AIN pellet sintered	4	73	
AIN thin film deposited on fused silica	8	6.7	
AIN thin film deposited on stainless steel	4	14.2	

#### 4.0 Conclusion

Piezo electric sensors for use at harsh environment is needed for structural health monitoring of advanced nuclear reactor fleet. AIN is a good piezo electric material for use at harsh environment for a variety of excellent thermophysical properties. Integration of AIN to a structural alloy is challenging because it involves joining a non-oxide ceramic to metal. This study looked at growing AIN phase in-situ within candidate structural alloys. Heat treatment of FeCrAl under N<sub>2</sub> environment leads to AIN formation. PFM measurement shows presence of piezo response in areas within FeCrAl that contains AIN. This method needs further investigation to come up with larger quantity of AIN phase and control the crystal orientation of in-situ grown AIN phase.

Conclusion 13

#### 5.0 References

- 1. Reinhardt, B., J. Daw, and B. R. Tittmann. "Irradiation Testing of Piezoelectric (Aluminum Nitride, Zinc Oxide, and Bismuth Titanate) and Magnetostrictive Sensors (Remendur and Galfenol)." *IEEE Transactions on Nuclear Science* 65, no. 1 (2018): 533-538.
- 2. Reinhardt, B. T., A. Suprock, and B. Tittmann. "Testing Piezoelectric Sensors in a Nuclear Reactor Environment." *AIP Conference Proceedings* 1806, no. 1 (2017): 050005.
- 3. Rempe, J. D., D. Knudson, R. Schley, L. Bond, J. Coble, M. Good, and R. Meyer. *In-pile Instrumentation to Support Fuel Cycle Research and Development FY11 Status Report*. INL/EXT-11-23119, Revision 0. Idaho National Laboratory, 2011.
- 4. Fei, C., X. Liu, B. Zhu, D. Li, X. Yang, Y. Yang, and Q. Zhou. "AlN Piezoelectric Thin Films for Energy Harvesting and Acoustic Devices." *Nano Energy* 51 (2018): 146-161.

References 14

## Pacific Northwest National Laboratory

902 Battelle Boulevard P.O. Box 999 Richland, WA 99354

1-888-375-PNNL (7665)

www.pnnl.gov